High-Gain, Long-Pulse Free-Electron-Laser Oscillator

J. Mathew[a] and J. A. Pasour
Naval Research Laboratory, Washington, D. C. 20375
(Received 8 January 1986)

We report the first operation of a high-gain, long-pulse (>1 μsec), free-electron-laser oscillator. The growth rate is measured by variation of the interaction length of the electron beam within the oscillator cavity. The observed power gain per pass of up to 10^4 and the buildup of cavity power to multimegawatt levels are in agreement with high-gain oscillator theory. Growth rates have also been measured as a function of wiggler field strength.

PACS numbers: 42.55.Tb

During the past few years, several free-electron-laser (FEL) devices have been successfully operated.[1] These devices have operated as amplifiers in both the high-gain and low-gain regimes, as high-gain superradiant amplifiers, or as low-gain oscillators. For some applications, and especially at frequencies where input sources are not available, it would be desirable to have a long-pulse-duration, high-power oscillator. A steady-state oscillator requires a beam duration many times longer than a radiation transit time in the resonator, and a high-gain, high-power device requires a large beam current. Previous attempts[2,3] to study high-gain oscillators have been difficult because the electron pulse duration was only a few times longer than a radiation transit time. Long-pulse FEL oscillators utilizing 1–10-A electron beams have been reported,[4,5] but at much lower gain and power levels.

In this Letter, we present initial results of a high-gain FEL oscillator driven by an induction linac having a 2-μsec pulse duration, approximately 200 times longer than the radiation transit time. The power gain per pass is as large as 10^4, and the device operates in the *Ka* band ($f=25$–40 GHz) at the multimegawatt level. Growth rates have been measured by variation of the interaction length, and the observed exponential growth is in excellent agreement with a recent high-gain oscillator theory.[6] Several types of resonators have been tested, and a wide range of experimental parameters have been used.

The FEL oscillator is shown schematically in Fig. 1. The electron beam from the induction linac[7] enters the oscillator through an aperture and a microwave reflector which is positioned just outside the wiggler. The electron beam energy has been varied from ~ 400 to ~ 600 keV, and the beam current entering the wiggler has been varied from 50 to 300 A by the changing of apertures. The wiggler is a bifilar helix having a period $\lambda_w = 4$ cm and a 6-period-long adiabatic entry and exit. The constant-amplitude portion of the wiggler is 22 periods long, and the field on axis can be varied up to 1 kG. The electron beam is focused solely by the wiggler field, and so no axial magnetic field is employed.[8] The electrons are dumped to the wall of the 3-cm-diam waveguide before they reach the output mirror. The radiation coupled out through the output mirror is radiated from the system through a conical horn and vacuum window.

We have tested several different types of reflectors for the input and output mirrors. Ideally, the input mirror should not perturb the electron beam. Consequently, we have employed either a Bragg reflector,[3,9] as shown in Fig. 1, or an aperture reflector. The copper Bragg reflector is a section of circular waveguide having seven rectangular corrugations, each 2 mm deep $\times$ 9 mm wide. The aperture reflector is a 1.27-cm-diam beam aperture which is reversed from the position shown in Fig. 1 so that a sharp step forms the resonator boundary. Both reflectors have power reflection coefficients $R \approx 65\%$, but the Bragg reflector only operates over a narrow frequency band (31.7 ± 0.3 GHz for the TE_{11} mode). The output mirror is either a copper plate with a 0.6-cm-diam hole on axis ($R \approx 96\%$), a copper plate having an array of 0.15-cm-diam holes ($R > 99\%$), or a fine, woven tungsten mesh which has been copper plated ($R \approx 60\%$).

We vary the interaction length of the beam within the oscillator cavity by positioning a dump coil (shown schematically in Fig. 1) at appropriate locations along the wiggler. This coil is connected in series with the wiggler and produces a transverse magnetic field 2.2 times stronger than the wiggler field on axis. This deflecting field is localized over a 5-cm length of the wiggler, and the entire beam is typically dumped to the waveguide wall within a distance of about 3 cm. We

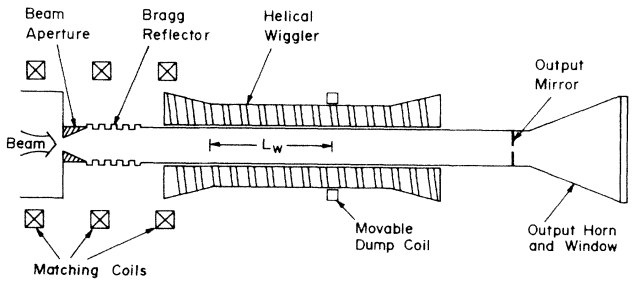

FIG. 1. Schematic diagram of experiment.

have also verified (by using scintillator photographs) that the beam is well defined and unaffected until it reaches the edge of the dump coil.

Because the wiggler employs an adiabatic entrance section, the effective interaction length, L_w, is assumed to be 20 cm less than the total length of the wiggler before the dump coil. We estimate that this assumed value of L_w may differ from the actual interaction length by ± 2 cm. As we increase the interaction length by changing the position of the dump coil, we observe a sharp threshold for oscillation. The threshold interaction length, L_{th}, varies from 20 to 60 cm, depending on the experimental parameters. In general, we observe no radiation when $L_w < L_{th}$; but if $L_w \gtrsim L_{th} + 2$ cm, the output power saturates at a level nearly independent of L_w.

The output power is typically monitored with a crystal detector at the end of a calibrated attenuator chain. Shown in Fig. 2 are oscilloscope traces of the beam current entering the wiggler together with the crystal detector signal for several different situations. We define the turn-on time τ as the delay between the time at which the transmitted beam current reaches 90% of its peak, and the time when microwave power is detected. The power level at turnon is ~ 15 dB below the saturation level, which varies from 1 to 10 MW depending on the parameters. The choice of 90% of peak current as the beginning of the interaction is somewhat arbitrary. The interaction could possibly begin 40 nsec earlier or later than this time.

The turnon time greatly decreases as L_w is increased, as can be seen in Fig. 2. This effect can be understood if one recognizes that for $L_w < L_{th}$, the single-pass power gain is less than the losses, which are primarily due to mirror transmission at the ends of the cavity. When $L_w > L_{th}$, there is a net positive gain G per pass. On the assumption that the interaction time is long enough, the power level will eventually reach saturation. Of course, a much longer time is required when L_w only slightly exceeds L_{th} and G is small than when $L_w >> L_{th}$ and G is large.

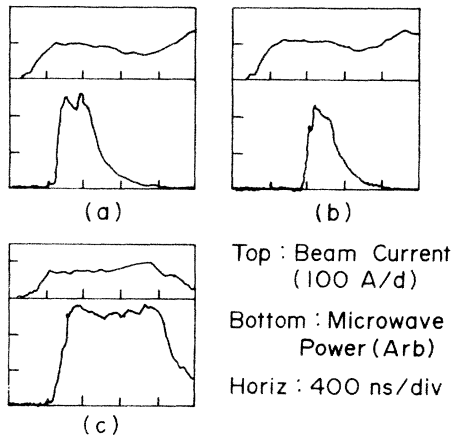

FIG. 2. Oscillograms of beam current in the wiggler and microwave output with $B_w = 613$ G. (a) Mesh reflector, $L_w = 74$ cm. (b) Mesh reflector, $L_w = 32$ cm. (c) Perforated copper plate reflector, $L_w = 70$ cm.

Another interesting phenomenon is apparent in Fig. 2. The microwave pulse is quite short when the mesh filter is used as the output mirror, but the pulse is much longer with the copper plate reflector. By using open-shutter photography, we have observed breakdown on the mesh reflector due to the high-power microwaves, even though the base pressure in the wiggler cavity is 2×10^{-6} Torr. No breakdown is observed with the copper plate reflector, and the device operates in a steady state. There are occasions when the output pulse is short even with the copper plate reflector, and we have some evidence that this is due to plasma formation in the waveguide, possibly when the beam strikes the wall. Because the breakdown occurs after saturation, it does not affect the determination of growth rate. In fact, our most complete set of growth rate data has been obtained with the mesh reflector and will be presented here, but comparable growth rates have been measured with the copper plate reflectors.

A recently developed theory[6] treats the case of power buildup in a high-gain FEL oscillator. For times longer than a round-trip time, the cavity power is given by

$$P = P_0 \exp\{2[\Gamma L_w - \ln(n/\sqrt{R})]t/\tau_b\}, \quad (1)$$

where P_0 is the spontaneous radiation power level, Γ is the linear electric field growth rate, $1-R$ is the round-trip power loss in the resonator, $\tau_b \approx 2L/c$ is the round-trip bounce time, and L is the cavity length (178 cm for the data presented). The factor of n inside the logarithm represents the coupling loss due to the splitting of the radiation into n modes, only one of which grows.[6] In the Raman regime, $n=2$; but in the high-gain Compton or strong-pump regime, $n=3$.

From Eq. (1) it is obvious that net gain will occur only when $\Gamma L_w > \ln(n/\sqrt{R})$. The experimentally determined value of L_{th} is the minimum L_w for which gain is observed. Consequently, we have

$$\Gamma = L_{th}^{-1} \ln(n/\sqrt{R}). \quad (2)$$

The growth rate determined from Eq. (2) can of course be compared with theoretical expressions or simulations. However, this only checks the validity of Eq. (1) at a single point ($L_w = L_{th}$). To obtain a more thorough test of Eq. (1), we rewrite it as

$$\tfrac{1}{2}\ln(P_t/P_0) = (L_w N_b)\Gamma - N_b \ln(n/\sqrt{R}), \quad (3)$$

where we have defined P_t as the power level at turnon time τ and $N_b = \tau/\tau_b$. Strictly speaking, Eq. (1) was derived under conditions that required N_b to be an in-

teger. However, since $N_b >> 1$ for most of the data in this paper, we choose to treat N_b as a continuous variable.

From Eq. (3) we see that if Γ and R are constants and if the power grows exponentially as specified by Eq. (1), then a plot of $L_w N_b$ vs B_b must be a straight line with slope $\Gamma^{-1}\ln(n/\sqrt{R})$. Moreover, in the limit $N_b \to 0$, the intercept on the $L_w N_b$ axis provides $(\frac{1}{2}\Gamma)\ln(P_t/P_0)$. Even though the ratio P_t/P_0 may not remain constant from shot to shot, the weak logarithmic dependence on P_t/P_0 makes the left-hand side of Eq. (3) very nearly a constant.

Shown in Fig. 3 is a plot of $L_w N_b$ vs N_b, obtained with the mesh output reflector. The circles represent the data as calculated by use of the definitions of L_w and N_b given above. A straight line having a slope of 25.3 cm fits these data quite well. Also shown are the points as calculated by use of the maximum uncertainties in our definitions of L_w and τ. For $N_b < 10$, the data are very sensitive to the definition of τ. The large deviation of the squares and triangles from a straight line for $N_b < 10$ and the good fit of the circles indicate that our time definition is probably much better than ± 40 nsec. Nevertheless, if we continue to use this uncertainty, the resulting slopes (dashed lines in the figure) for $N_b > 10$ are 22.3 and 27.6 cm, respectively.

To determine the growth rate experimentally by use of this approach, the operating regime must be known.[10,11] In order to operate in the Raman regime,[11] we must have

$$B_w < mc^2[\pi\omega_p/(F\lambda_w\gamma^{3/2}c)]^{1/2}/e,$$

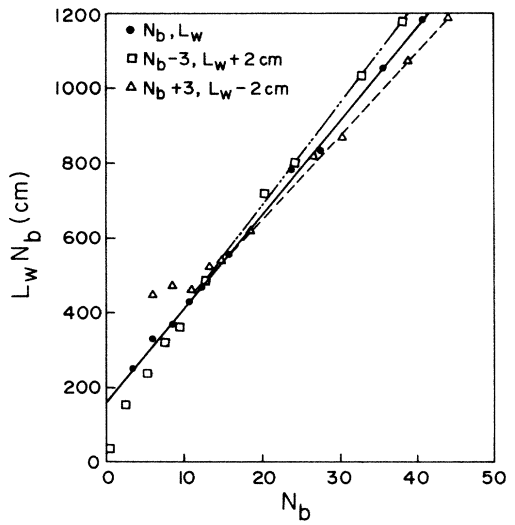

FIG. 3. $L_w N_b$ vs N_b, where N_b is the number of radiation bounce times required for power buildup. The squares and triangles correspond to the maximum systematic uncertainties in L_w and N_b. The resonator consists of a mesh output reflector and a 0.6-cm-diam aperture input reflector. $B_w = 613$ G.

where F is the beam filling factor and ω_p is the electron plasma frequency. With the experimental parameters for the data in Fig. 3, this transition wiggler field is ≈ 1.2 kG. Consequently, the interaction is expected to be in the Raman region, and so we take $n = 2$. Then the line slopes in Fig. 3 together with the measured reflectivity give $\Gamma = 0.047 \pm 0.005$ cm. This value of Γ together with the intercept on the $L_w N_b$ axis provides $P_t/P_0 \sim 10^7$, which is quite reasonable.

We can also calculate Γ from Eq. (2) if $L_{\rm th}$ is experimentally determinable. Strictly speaking, $L_{\rm th}$ represents the interaction length required for the radiation to grow by an infinitesimal amount over the spontaneous noise level. Experimentally, we observe $L_{\rm th} = 28.5$ cm. However, this value is approximate because the radiation must grow from noise by $\sim 10^7$ within a time $t/\tau_b = 120$ in order to be detectable. The importance of this approximation can easily be determined. Using Eq. (2) with $n = 2$ and $L_{\rm th} = 22.5 \pm 2$ cm gives $\Gamma = 0.041 \pm 0.003$ cm^{-1}. Alternatively, setting $P/P_0 = 10^7$, $L_w = 28.5$ cm, and $t/\tau_b = 120$ in Eq. (1), we obtain $\Gamma = 0.043$ cm^{-1}. Consequently, because of our long-duration beam pulse, this effect is not very important. It is therefore possible to determine Γ from Eq. (2), and the result agrees quite well with the value from Fig. 3.

If we take into account the uncertainties in the beam energy, transmitted current, filling factor, and beam radius, the cold-beam theory[10] gives $0.03 < \Gamma < 0.06$ for the Raman regime. Three-dimensional numerical simulations of the experiment have been performed by Freund[12] using an amplifier code which treats waveguide modes. The simulations give $\Gamma \approx 0.05$ cm^{-1} for the TE_{11} mode, which is the mode we observe. Consequently, the data agree very well with both theory and simulation. Oscillator simulations are beginning to be carried out, and the results will be reported in the future.[13]

The functional dependence of growth rate on wiggler magnetic field provides additional information about the regime in which the FEL is operating. Theoretically, in the Raman regime $\Gamma \propto B_w$. The experimentally observed wiggler field dependence is shown in Fig. 4, as calculated with $n = 2$. Superposed on the experimental data is the theoretical scaling curve for the Raman regime. Because of uncertainties in calculation of the absolute theoretical growth rates, we have chosen to verify only the functional dependence of the growth rate on the wiggler field strength. We have therefore arbitrarily chosen the best fit to the data for the scaling curve. No error bars are shown because the systematic errors simply shift all the points up or down by nearly the same amount (≤ 0.005 cm^{-1}). The errors due to shot-to-shot variations are represented by the size of the data points.

A comparison of the experimental data and theoreti-

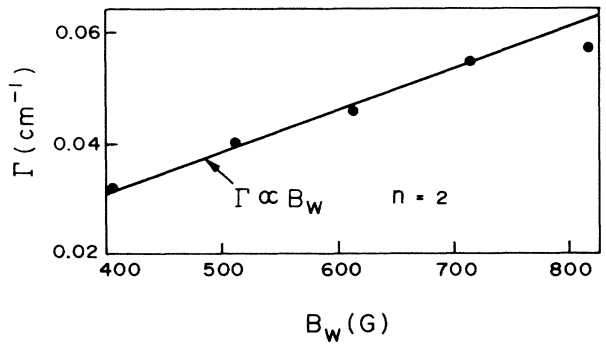

FIG. 4. Experimentally determined growth rate vs wiggler field on axis. The experimental configuration is identical to that for Fig. 3. Also shown is the theoretical scaling curve for the Raman regime.

cal curve in Fig. 4 shows that when $B_w < 700$ G, the linear dependence is excellent. The "saturation" of growth rate for $B_w > 725$ G might be caused by the operating regime of the FEL shifting more towards the high-gain Compton region, where $\Gamma \propto B_w^{2/3}$. It is also partially due to a deterioration of beam transport inside the oscillator cavity at higher wiggler fields.

In conclusion, a high-gain, long-pulse, steady-state FEL oscillator has been operated. We have demonstrated a simple, effective technique for the unfolding of high-gain FEL oscillator growth rates. The observed exponential growth is in agreement with high-gain oscillator theory and 3D simulations. The dependence of the measured growth rate on the wiggler field strength is consistent with operation in the Raman regime for most of the parameter range studied.

We thank S. Krafsig and R. Covington for assistance in operating the experiment. We also wish to thank Dr. C. A. Kapetanakos, Dr. P. Sprangle, Dr. C. M. Tang, and Dr. H. Freund for helpful discussions and comments. This work was supported by the Office of Naval Research and the Strategic Defense Initiative Organization.

[a]Presently at Sachs/Freeman Associates, Landover, Md. 20785.

[1]See, e.g., Third Special Issue on Free-Electron-Lasers, edited by V. L. Granatstein and C. W. Roberson, IEEE J. Quantum Electron. **21**, 804–1113 (1985).

[2]D. B. McDermott *et al.*, Phys. Rev. Lett. **41**, 1368 (1978).

[3]V. L. Bratman, G. G. Denisov, N. S. Ginzburg, and M. I. Petelin, IEEE J. Quantum Electron. **19**, 282 (1983).

[4]M. Z. Caponi, J. Munch, and H. Boehmer, in *Free-Electron Generators of Coherent Radiation,* edited by S. Jacobs *et al.*, Physics of Quantum Electronics Vol. 7 (Addison-Wesley, Reading, Mass., 1950), pp. 523–554.

[5]L. R. Elias, J. Hu, and G. Ramian, Nucl. Instrum. Methods Phys. Res., Sect. A **237**, 203 (1985).

[6]W. P. Marable, P. Sprangle, and C. M. Tang, in Proceedings of the Seventh International Free-Electron Laser Conference, September 1985 (to be published).

[7]J. E. Leiss, N. J. Norris, and M. A. Wilson, Part. Accel. **10**, 223 (1980).

[8]J. A. Pasour, R. F. Lucey, and C. A. Kapetanakos, Phys. Rev. Lett. **53**, 1728 (1984).

[9]R. J. Harvey and F. A. Dolezal, in Proceedings of the Seventh International Free-Electron Laser Conference, September 1985 (to be published).

[10]P. Sprangle, R. A. Smith, and V. L. Granatstein, in *Infrared and Millimeter Waves,* edited by K. J. Button (Academic, New York, 1979), Vol. 1, pp. 279–327.

[11]N. M. Kroll and W. A. McMullin, Phys. Rev. A **17**, 300 (1978).

[12]H. Freund, private communication; A. K. Ganguly and H. P. Freund, Phys. Rev. A **32**, 2275 (1985).

[13]W. P. Marable and C. M. Tang, private communication.